THE GENETIC BASIS OF INTER-ISLAND MATING BEHAVIOR DIVERGENCE

Running title: mating behavior genetics in *Laupala*

Thomas Blankers[1], Kevin P. Oh[1], Kerry L. Shaw[1]

Department of Neurobiology and Behavior, Cornell University, Ithaca, NY, USA.

For correspondence: W319 Mudd Hall, 215 Tower rd, Ithaca, NY. thomasblankers@gmail.com

AUTHOR CONTRIBUTIONS

TB, KPO, and KLS conceived the study, KPO conducted the experiments, TB analyzed the data, and TB and KLS wrote the manuscript with input from KPO.

ACKNOWLEDGEMENTS

We would like to thank Jon Lambert for sample collection and RNA extraction, Michael Brewer for assistance with transcriptome sequencing, Aureliano Bombarely for help with the bioinformatic analyses that contributed to the transcriptome assembly, and Dr Chenowith and two anonymous reviewers for helpful comments that improved an earlier version of the manuscript. We thank the Shaw Lab, and especially Mingzi Xu, for valuable discussions of methodology. Furthermore, we acknowledge Karl Broman and the R/QTL discussion group as well as the Biostars and Stackoverflow communities for help with the analyses. This work was supported by the National Science Foundation grant number IOS1257682 "The Genomic Architecture underlying Behavioral Isolation and Speciation'. The authors declare no conflict of interest.

DATA ACCESIBILITY

Scripts will be made available on github.com/thomasblankers/CerEukQTL. The transcriptome and RNAseq reads will be made available on NCBI's GenBank under BioProject number PRJNA429662. The Genotype-by-sequencing data will be made available under BioProject number PRJNA429815. All other data that have not been attached in the supplementary material will be made available in a Dryad repository.

ABSTRACT

Mating behavior divergence is a major source of reproductive isolation and an important force driving speciation in various biogeographic contexts. However, the relationship between biogeographic history, the tempo and mode of speciation, and the genetic architecture of speciation phenotypes is poorly understood. Here, we use quantitative trait locus (QTL) mapping to infer the number, distribution, and effect size of song rhythm variation in the crickets *Laupala eukolea* and *L. cerasina*, which occur on different islands (Maui and Hawai'i). We then compare these results with a similar study of an independently evolving species pair that diverged within the same island. Pulse rate divergence is associated with a polygenic genetic architecture in both the intra- and inter-island species pair. We find evidence consistent with parallel genetic differentiation and a relationship between magnitude of phenotypic divergence and number of causal loci. Functional annotation and GO enrichment showed that QTL regions identified here are enriched for homologs of genes with known function in pathways that may be involved in modulating cricket song rhythm. This is consistent with tightly-linked clusters of functionally related genes in QTL regions and reveals several candidate genes that merit further study.

Keywords: speciation, sexual isolation, quantitative genetics, transcriptome, *Laupala*

INTRODUCTION

Behavioral (sexual) isolation is a major reproductive barrier in animals and an important force driving speciation (Mayr 1963; West-Eberhard 1983; Ritchie and Phillips 1998; Coyne and Orr 2004). However, the genetic mechanisms leading to sexual trait divergence, suppression of interspecific recombination, and ultimately the origin of new species remain poorly understood (Ritchie and Phillips 1998; Mackay 2001; Boake et al. 2002; Hoekstra 2010). We can make significant progress in understanding the speciation process by providing empirical insight into the genetic architecture of mating behavior divergence – the number, effect size, and genomic distribution of causal loci – as well as identifying the genes controlling divergent sexual behaviors.

The genetic architecture of phenotypes can be categorized as Type I (polygenic, additive) or Type II (oligogenic, epistatic) architectures (Templeton 1981). It has been argued that the type of genetic architecture can be informative about the tempo and mode of speciation (Carson and Templeton 1984; Harrison 1991). All else being equal, an oligogenic basis would allow for rapid phenotypic evolution, because the phenotypic effect of a single mutation is expected to be larger; theoretical models for sexual selection often assume such simple genetic architectures (Dieckmann and Doebeli 1999; Gourbiere 2004; Doorn et al. 2009; Servedio and Burger 2014). Moreover, it has also been suggested that oligogenic architectures may be lynch pins in radiations involving founder effects (Carson and Templeton 1984), such as those accompanying the colonization of archipelagos. In contrast, empirical studies show that divergent sexual traits are typically associated with Type I genetic architectures (Ritchie and Phillips 1998; Chenoweth and McGuigan 2010), without a disproportionate contribution from sex-linked loci (Ritchie and Phillips 1998; Qvarnström and Bailey 2009); although, the role of X-effects on the evolution of

70 secondary sexual characters remains somewhat contentious (e.g., Mittleman et al. 2017). A
71 polygenic architecture would allow for gradual (but not necessarily slow) and orchestrated
72 divergence of male and female sexual traits (Lande 1981; Shaw and Parsons 2002).

73 Another aspect of the genetic architecture that can greatly affect the rate of trait evolution is the
74 clustering of functionally related genes in specific genomic regions (also known as
75 "supergenes"). Fisher (1930) suggested that genes associated with the gradual adaptive change of
76 complex phenotypes become physically linked over time. He imagined this linkage would
77 maintain the identity of groups with complex phenotypic differences by reducing the disruptive
78 effects of recombination in the region with which the phenotype is associated. Indeed, linkage
79 disequilibrium within tightly linked clusters of quantitative trait loci (QTL) can be maintained by
80 low recombination (Noor et al. 2001).

81 The involvement of gene clusters has been implicated in the rapid evolution of (co)adaptive
82 phenotypes in plants and animals (Schwander et al. 2014), including courtship behavior (Gould
83 et al. 2010; Küpper et al. 2015; Lamichhaney et al. 2015; Tuttle et al. 2016). When functionally
84 relevant genes are closely linked (comprising co-adapted gene complexes), orchestrated adaptive
85 responses may be greatly facilitated: mutually beneficial and co-dependent alleles can segregate
86 as a single unit and recombination between forms rarely produces maladaptive allelic
87 combinations. This may be an important mechanism constraining natural variation in complex
88 traits, such as altruistic signals ('green beard', Dawkins 1976) or the interconnected properties of
89 the neural circuitry that control behaviors, including sex-specific mating behaviors, for which
90 male and female traits need to co-evolve within the population (Fisher 1930; Lande 1981;
91 Kirkpatrick and Ravigne 2002).

92 Here, we infer the number and distribution and predict the function of loci involved in sexual
93 trait divergence between two species of the endemic Hawaiian cricket genus *Laupala*.
94 Differentiation in acoustic sexual signaling behavior appears to play a central role in *Laupala*
95 speciation, a group with one of the highest speciation rates documented for arthropods
96 (Mendelson and Shaw 2005). Species are endemic to single islands and show striking
97 differentiation in male song and female (song) preference (Otte 1994; Mendelson and Shaw
98 2005). Like most other cricket species, the male produces a song by rubbing together its
99 specialized forewings. The songs of *Laupala* crickets are relatively simple and consist of trains
100 of pulses, each produced by a single closing movement of the wings. Evidence suggests that a
101 critical trait used in female mate choice is the repetition rate of these pulses, i.e. the pulse rate
102 (Alexander 1962; Otte 1992), which is highly heritable and constitutes one of the major sources
103 of phenotypic divergence among *Laupala* species (Shaw 1996, 2000; Grace and Shaw 2011; Oh
104 et al. 2012; Oh and Shaw 2013).

105 The neurobiology of cricket song generation is generally well understood. The major structures
106 controlling the cricket song rhythm are the descending brain neurons and specialized motor
107 neurons in the thorax, called central pattern generators (Hennig and Otto 1996; Hedwig 2014;
108 Schöneich and Hedwig 2017). A wide variety of neurological cell types, ion channels,
109 neurotransmitters, and hormonal neuromodulators are expected to contribute to the rhythmic
110 properties of pattern generators (Marder and Bucher 2001) and to the song rhythm in crickets
111 (Gerhardt and Huber 2002; Hedwig 2014). So far, we have not been able to pin cricket song
112 rhythm variation down to individual genes, but other organisms with known genetic and
113 neurological pathways that drive sex-specific and (acoustic) courtship behaviors can shed light
114 on the potential mechanisms. In *Drosophila melanogaster*, sexual dimorphism in the nervous

115 system, which forms the basis of courtship song neurobiology, is controlled by the sex-specific
116 transcription factor *fruitless* in interaction with *doublesex* (Clyne and Miesenböck 2008;
117 Yamamoto and Koganezawa 2013). However, neither of these genes contributes to interspecific
118 differences in song rhythm (Cande et al. 2014). Two other genes, *slowpoke* and *cacophony*, have
119 been implicated in species and population differences across *Drosophila* species: these genes
120 control the properties of ion (calcium and potassium) channels at neuromuscular junctions
121 (Gleason 2005; Etges et al. 2007; Veltsos et al. 2015) and can transform the output of neuronal
122 networks including central pattern generators (Crocker et al. 2010). Therefore, we may expect
123 similar neuromodulators as well as genes involved in synaptic transmission at neuromuscular
124 junctions and rhythmic behavior to contribute to variation in song rhythm in crickets.

125 The first goal of this study is to illuminate the genetic architecture of sexual trait divergence in
126 the light of different geographical modes of speciation. There is evidence from a biometric study
127 that multiple genetic factors (~5) contribute to pulse rate variation in *L. cerasina* and *L. eukolea*
128 (Oh et al. 2012) despite rapid phenotypic divergence following colonization of a new island
129 (Mendelson et al. 2004). We thus hypothesize that pulse rate divergence is associated with a
130 polygenic architecture, independent of the biogeographic mode of speciation. Using quantitative
131 trait locus (QTL) mapping we examine the number, effect size, and genomic distribution of loci
132 contributing to interspecific pulse rate variation in *L. cerasina* and *L. eukolea*. We then discuss
133 these results in the light of an earlier study dissecting the genetic architecture of pulse rate
134 divergence in *L. kohalensis* and *L. paranigra* (Shaw et al. 2007), an independently evolving
135 species pair which has diverged within a single island (Hawai'i; Otte 1994; Mendelson and Shaw
136 2005).

137 The second aim of this study is to examine the genomic arrangement of the genes controlling
138 mating behavior divergence in this system. We test the hypothesis that the functionally related
139 genes are clustered in QTL regions. Using genome-wide, functional genetic data from both sexes,
140 and across ontogenetic stages and reproductive states, we annotate the genetic map and associate
141 the segregating loci with Gene Ontology terms. Based on theoretical predictions (Fisher 1930) as
142 well as empirical findings for mating behavior genetics in birds (Küpper et al. 2015;
143 Lamichhaney et al. 2015) and moths (Gould et al. 2010), we predict that QTL regions contain
144 multiple, functionally related genes. Given the involvement of genes controlling ion channels at
145 the neuromuscular junctions and other neuromodulators in song variation in *Drosophila*, we
146 expect QTL regions to be enriched for genes with putative functions in neuromuscular processes
147 associated with song production, rhythmic behaviors, or mating behavior. This would suggest
148 that functionally related genes cluster inside QTL regions (rather than that a QTL region harbors
149 a single gene driving the observed phenotypic effect).

150 **MATERIAL & METHODS**

151 All custom R scripts as well as all commands in Linux and Python used in the analyses described
152 above will be made available in the supplementary information.

153 *Samples and interspecific crosses*

154 *Laupala eukolea* nymphs were collected in 2012 in Kipahulu Valley on Maui at Ginger Camp
155 (20º 41’ 60.000’’ N; 156º 5’ 18.000’’ W) and Palikea Peak (20º 40’ 20.640’’ N; 156º 4’ 5.160’’
156 W); *L. cerasina* were collected in Kalopa State Park (20º 2’ 13.200’’ N; 155º 26’ 36.960’’ W) on
157 Hawai’i Island. Animals were kept in the lab in plastic cups under constant temperature (20º) and
158 humidity, and were provided cricket chow (Fluker Farms, LA) *ad libitum* as well as substrate to
159 lay eggs. Males and females were kept separately to ensure virginity of all animals. They were

160 phenotyped between two and ten weeks after the final molt, during which sexual receptivity is
161 maximized in *Laupala* (Grace and Shaw 2011). Two families of first generation interspecific
162 hybrids (HC1 & HC2) were each generated by mating a *L. cerasina* male with a *L. eukolea*
163 female. Several males and females from each family (14 full sib pairs from each of the families)
164 were used to obtain second generation hybrids following the breeding design in (Shaw 1996).

165 *Phenotyping*

166 Male songs were recorded following the methods in (Shaw, 1996). A single recording for each
167 individual (*L. cerasina*, n = 24; *L. eukolea*, n = 16; F2, n = 230) was made between 10 A.M. and
168 4 P.M. Virgin, adult males were recorded individually in a plastic container with screen covers in
169 an anechoic and temperature-controlled chamber using a SONY Pro Walkman cassette recorder
170 and SONY microphone. Songs were then digitized using SOUNDSCOPE/16 (GWI Instruments,
171 Cambridge, MA, USA) at 44.1 kHz to generate an oscillogram displaying trains of pulses
172 (singing bouts). We estimated the pulse rate by averaging the inverse of five pulse periods
173 (measured from the onset of a pulse to the onset on the next pulse) measured from a single
174 singing bout.

175 *Genotyping*

176 We extracted DNA from whole adult crickets using the DNeasy Blood & Tissue Kits (Qiagen,
177 Valencia, CA, USA). Genotype-by-Sequencing library preparation and sequencing were done in
178 2014 at the Genomic Diversity Facility at Cornell University following Elshire et al. (2011). The
179 *Pst* I restriction enzyme was used for sequence digestion and DNA was sequenced on the Illumina
180 HiSeq 2000 platform (Illumina Inc., USA) with 100 bp single end reads.

181 Reads were trimmed and demultiplexed using Flexbar (Dodt et al. 2012) and then mapped to the
182 *L. kohalensis de novo* draft genome using Bowtie2 (Langmead and Salzberg 2012) with default
183 parameters. We then called SNPs using two different pipelines: The Genome Analysis Toolkit
184 (GATK; DePristo *et al.* 2011; Van der Auwera *et al.* 2013) and FreeBayes (Garrison and Marth
185 2012). For GATK we used individual BAM files to generate gVCF files using 'HaplotypeCaller'
186 followed by the joint genotyping step 'GenotypeGVCF'. We then evaluated variation in SNP
187 quality across all genotypes using custom R scripts to determine appropriate settings for hard
188 filtering based on the following metrics (based on the recommendations for hard filtering section
189 "Understanding and adapting the generic hard-filtering recommendations" at
190 https://software.broadinstitute.org/gatk/ accessed on 28 February 2017): quality-by-depth, Phred-
191 scaled *P*-value using Fisher's Exact Test to detect strand bias, root mean square of the mapping
192 quality of the reads, u-based z-approximation from the Mann-Whitney Rank Sum Test for
193 mapping qualities, u-based z-approximation from the Mann-Whitney Rank Sum Test for the
194 distance from the end of the read for reads with the alternate allele. For FreeBayes we called
195 variants from a merged BAM file using standard filters. After variant calling we filtered the
196 SNPs using 'vcffilter', a Perl library part of the VCFtools package (Danecek et al. 2011) based
197 on the following metrics: quality (> 30), depth of coverage (> 10), and strand bias for the
198 alternative and reference alleles (SAP and SRP, both > 0.0001). Finally, the variant files from the
199 GATK pipeline and the FreeBayes pipeline were filtered to only contain biallelic SNPs with less
200 than 10% missing genotypes using VCFtools. We retained all SNPs that had identical genotype
201 calls between the two variant discovery pipelines. We then pruned our data further to contain
202 only ancestry informative markers (i.e. grandparents are homozygous for alternative alleles), one
203 SNP per scaffold, markers with no or only limited segregation distortion (χ^2- square associated q-

204 value ≤ 0.05, i.e. a 5% false discovery rate [Benjamini & Hochberg, 1995]), and markers with
205 fewer than 99% of their genotypes in common with other marker loci (i.e. exclude one of each
206 pair of marker loci with identical genotypes for all individuals).

207 *Linkage mapping*

208 To infer the genetic architecture, we first performed a QTL scan to detect the number, effect size
209 and any possible interactions of the regions associated with variation in pulse rate. For each of
210 the hybrid cross families, HC1 and HC2, we created linkage maps separately using MapMaker
211 (Lander et al. 1987). Map construction followed four steps. First, markers were grouped into
212 linkage groups using the 'group' command with the 'default linkage criteria' set to 4.0 (LOD)
213 and 35 (cM). Second, for each group, a subset of the marker passing a series of quality criteria,
214 i.e. informative, well-spaced markers, were ordered using the 'order' command. Markers were
215 considered informative if they had no missing genotypes and well-spaced if they were more than
216 2.0 cM apart from other markers. Third, remaining markers were added with the 'build'
217 command and the order was verified using the 'ripple' command. Markers were first added to the
218 map satisfying a log-likelihood threshold of 4.0 for the positioning of the marker (i.e., the
219 assigned marker position is 10,000 x more likely than all other positions), then adding remaining
220 markers at a log-likelihood threshold of 3.0, followed by a final step with log-likelihood
221 threshold set to 2.0. Markers not incorporated into the map at this stage were discarded. To
222 determine the final marker order we used the 'ripple' command with a window size of 6 markers
223 and a log-likelihood threshold of 2.0. Arbitrary orders in marker dense regions (i.e., orders with
224 similar likelihoods) were resolved using information from both HC1 and HC2 maps, choosing
225 the order that maximized the likelihood and minimized the map length (measured in cM) for
226 both cross families.

227 Fourth, and finally, the linkage maps were merged using the R package LPmerge (Endelman and
228 Plomion 2014). LPmerge uses linear programming to combine two maps from independent
229 populations based on the similarities in marker order. Incongruent marker orders between HC1
230 and HC2, i.e. linear inequalities, were solved based on the weight assigned to each independent
231 linkage map. The solution also depended on the size of the interval, *K*, in which conflicting
232 markers were detected and re-ordered (or removed if no solution was found and removing a
233 constraining marker improved the linear equality). For each linkage group separately, we varied
234 the weighting of the two linkage maps and the interval in which the linear inequality was
235 resolved (*K*) to find the consensus map associated with the lowest mean and variance of the root-
236 mean-squared error between the consensus map and the original maps.

237 *QTL mapping*

238 We used multiple-QTL models in the R/qtl (Broman et al. 2003) package to detect and locate
239 QTL and calculate effect sizes. For HC1 and HC2 independently, and for the merged (consensus)
240 map, we first performed a single QTL scan using the scanone function with the multiple
241 imputation method (Sen and Churchill 2001) and the Haley-Knot" regression (Haley and Knott
242 1992). We then performed a two-dimensional QTL scan using the Haley-Knott regression to
243 detect pairs of QTL and interaction effects among QTL. We then permutated the two-
244 dimensional QTL to establish penalized likelihood criteria for main and interaction effects. We
245 subsequently built a multiple QTL model, starting with the QTL with the highest LOD (log of
246 odds) score, refining the position using 'refineqtl', and then scanning for additional QTL. We
247 continued adding QTL (followed by refining their position) until an additional QTL did not
248 improve the LOD score of the model beyond the penalized LOD score threshold for main effects
249 at the alpha = 0.05 level. After the addition of each QTL, we checked for potential QTL

250 interactions that would improve the multiple QTL model beyond the (heavy) penalized LOD
251 score threshold for interaction effects at the alpha = 0.05 level. Finally, we estimated effect sizes
252 by fitting the QTL model and using the drop-one-term analysis. In the merged map, we included
253 cross type as a covariate in all steps described above. For comparison, we also used composite
254 interval mapping (CIM) to scan for QTL while using the markers under the QTL peaks identified
255 in the multiple QTL models as covariates and dropping those covariates if they were within a 20
256 cM window surrounding the tested region.

257 To estimate the true number of genetic loci underlying pulse rate variation based on the QTL
258 results, we use the method of Otto and Jones (2000). We first solved equation 11 (Otto and
259 Jones 2000) for zero, specifying a_{min} as the smallest QTL effect we detected in the QTL scan (for
260 HC1, HC2, or for the combined map) to calculate the threshold of the smallest QTL effect we
261 could detect. We then used equation 6 (Otto and Jones 2000) to estimate the true number of loci.
262 The calculations were done using custom function in R, which is available upon request and in
263 the Github repository associated with the manuscript.

264 *Transcriptome assembly*

265 To look for candidate genes in QTL regions and test for enrichment of specific gene functions
266 we first assembled the transcriptome to obtain information about putative gene function of the
267 loci within regions of interest. The *L. cerasina* individuals used for RNA-sequencing and
268 transcriptome assembly were first generation lab-reared offspring. A total of ten samples were
269 stored in RNAlater following the manufacturers recommendations (Qiagen, Germany) and
270 pooled by sex prior to sequencing: four adult males (two sampled in the morning and two
271 sampled in the evening, one of which was sampled immediately *after* mating a female), four
272 adult females (as with the males, two were sampled in the morning and the two were sampled in

273 the evening, one being collected immediately *after* mating), and a juvenile male and female. The
274 tissue was homogenized using sterilized forceps in RNAlater. RNA was extracted using the
275 RNAeasy kit (Qiagen, Germany). A quality check was done using a NanoDrop
276 spectrophotometer (Thermoscientific, Wilmington, DE, USA) and the Agilent Bioanalyzer 2100
277 (de Goor 2003). The samples were then sequenced on a single lane on the Illumina HiSeq 2000
278 platform with 50 bp paired end reads.

279 Reads were processed using Fastq-mcf from the Ea-Utils package (Aronesty 2011) with the
280 parameters -q 30 (trim nucleotides from the extremes of the read with qscore below 30) and -l 30
281 (discard reads with lengths below 30 bp). Read duplications were removed using PrinSeq
282 (Schmieder and Edwards 2011) and reads were corrected using Musket with the default
283 parameters (Liu et al. 2013).

284 We assembled the *L. cerasina* transcriptome using Trinity's (Haas et al. 2013) genome-guided
285 assembly pipline. We used the *Laupala kohalensis* reference genome (Blankers et al. 2017) and a
286 maximum intron size cut-off of 5000 bp. We first created a HISAT (Kim et al. 2015) index of the
287 genome and then aligned the male and female paired-end reads to the genome using default
288 settings. We sorted the resulting alignment SAM file and converted it to BAM format using
289 samtools (Li et al. 2009). We then did the genome-guided assembly using Trinity and checked
290 the quality of the assembly by calculating N50 statistics, mapping the male and female reads
291 back to the transcriptome using bowtie2 (Langmead and Salzberg 2012), and searching for
292 conserved eukaryote and arthropod genes from the BUSCO database (Simão et al. 2015). We
293 then mapped the reads back to the transcriptome using GMAP (Wu and Watanabe 2005) and
294 BLAT (Kent 2002), and used custom R scripts to retain a single best hit scaffold for each
295 transcript based on the coverage, identity, and number of matched bases.

296 *Transcriptome annotation*

297 We checked for contamination using NCBI's VecScreen, using the UniVec Core database and
298 the recommended blastn parameter values (https://www.ncbi.nlm.nih.gov/tools/vecscreen/about/,
299 accessed July 20 2017). We then functionally annotated the transcripts in three steps using
300 BLAST (Altschul et al. 1990; Camacho et al. 2009): first we matched our transcripts against the
301 *Drosophila melanogaster* proteome using an e-value cut-off of 1e-5. Any transcripts that were
302 not annotated in the first step were matched (at the same threshold) with the Uniprot/Swissprot
303 data base (The UniProt Consortium 2017), limiting our search to arthropod proteins. Finally, we
304 matched the remaining transcripts against the non-redundant protein database at NCBI, with an
305 e-value cut-off of 1e-5 and limiting our search to animal proteins.

306 We then used hmmer2go (https://github.com/sestaton/HMMER2GO) to estimate Open Reading
307 Frames (ORFs) and translated only a single, longest ORF per transcript. We annotated the
308 retained protein sequences using InterProScan (Zdobnov and Apweiler 2001; Jones et al. 2014).
309 We imported the transcriptome FASTA file, the XML output from the BLAST searches, and the
310 InterPro results into Blast2Go (Conesa et al. 2005). We recovered the original BLAST best hit,
311 and ran the Gene Ontology mapping using default settings. We then merged all these results and
312 ran the Annotation tool.

313 *Gene Ontology*

314 We tested the hypothesis that genes residing in QTL regions are functionally enriched for
315 biological processes potentially involved in cricket courtship behavior and song production. We
316 first used topGO from R's BioConductor environment (Alexa and Rahnenfuhrer 2016) to do
317 gene set enrichment analysis. We combined all the transcripts matching scaffolds within the

318 LOD 1 interval of the seven QTL peaks in the consensus linkage map (i.e. scaffolds with a
319 marker that explained pulse rate variation within a 1 LOD score significance level of the highest
320 LOD score for a given QTL). We then used the parent-child p-value correction (Grossmann et al.
321 2007) to test for GO term enrichment relative to the *L. cerasina* transcriptome. We did an
322 additional false discovery rate correction using the Benajamini & Hochberg algorithm
323 (Benjamini and Hochberg 1995) with the p.adjust function in R and considered any GO term
324 enriched within the QTL region at a false discovery rate of 10% or less. We also manually
325 inspected putative gene function in QTL regions by examining experimentally proven biological
326 and molecular functions for the highest ranked BLAST annotations on FlyBase (Gramates et al.
327 2017).

328 **RESULTS**

329 *Linkage mapping*

330 We mapped a total of 298 and 416 markers for HC1 (n=94) and HC2 (n=136), respectively (Fig
331 S1) to 8 linkage groups corresponding to the seven autosomes and the X chromosome in
332 *Laupala*. The map lengths were 821.2 cM and 734.1 cM corresponding to 2.72 marker/cM and
333 1.76 marker/cM, respectively. Merging the maps resulted in 508 unique markers at a total map
334 length of 776 cM (1.52 cM/marker).

335 *QTL mapping*

336 *Laupala cerasina* and *L. eukolea* males have non-overlapping, normally distributed pulse rate
337 distributions (Fig 1). The average pulse rate difference was 1.66 pulses per second (Table 1). The
338 F_2 song phenotype was normally distributed, the means of the HC1 and HC2 progeny did not

differ significantly ($P = 0.0724$), and the joint F2 distribution encompassed the parental species' phenotypic distributions (Table 1, Fig 1).

We detected two moderate effect (~10% of the species difference) QTL in both the HC1 and HC2 mapping populations on linkage group (LG) 1 and LG3 (Fig 2, Table 2). In HC2, we additionally detected three smaller effect QTL (< 5%) on LG5, LG7, and LGX. Merging the maps and combining the sample sizes also revealed a small effect QTL on LG2 and LG4 (Table 3). All (haploid) QTL effects were significantly larger than zero ($P < 0.05$) and of the same sign (Table 2, Table 3). Together, the seven QTL for the combined HC1 and HC2 mapping populations explained 38.73% (or 0.64 pps) of the phenotypic difference between the parental lines (Table 3; 20.18% and 32.07% for HC1 and HC2, respectively, Table 2). None of the QTL had significant dominant effects (Table S1) and no interactions of additive QTL were detected.

The QTL on LG1 and LG3 mapped to approximately the same location in HC1 and HC2, with the marker nearest to the peak in HC2 directly flanking the peak marker in HC1 (Fig 2, Table S2). Note that the genetic map of LG1 is substantially larger, indicating higher recombination rates in that region, in HC1 compared to HC2 and the combined map, but that this does not result in a different marker order. In general, the marker order on the linkage maps and mapped QTL intervals were highly concordant among the HC1, HC2, and combined map (Fig S1).

Based on the results for HC1 and HC2 and using the method in (Otto and Jones 2000) we estimated the true number of loci to be 9.41 (95% confidence interval = [1.57-29.02]; detection threshold, theta = 0.069 pps) and 8.84 (95% CI = [3.18-19.03]; theta = 0.018), respectively. Using all 230 F2 individuals, we estimated the true number of loci at 13.59 ((95% CI = [5.83-26.23]; theta = 0.025). The estimated amount of variation that remains undetected was ([true #

361 loci – detected # loci] x average effect size of undetected): [9-2] x 0.03 = 0.21 for HC1, [9-5] x
362 0.01 = 0.04 for HC2, and [14-7] x 0.01 = 0.07 for the combined map, respectively.

363 *Transcriptome*

364 We used the genome-guided assembly from the Trinity (Haas et al. 2013) pipeline to assemble
365 the transcriptome. Of the 50,148,157 reads after filtering (52,980,661 prior to filtering) that were
366 used to assemble the transcriptome, 90.58% mapped to the reference genome. The assembly had
367 a total length of 53,928,392 bp, the median contig length was 397 bp, and the contig N50 was
368 1,805 bp. Mean coverage was 49.9x and 40.8x for female and male reads, respectively. The male
369 and female reads mapped back to the transcriptome with high confidence, at mapping rates of
370 92.05% and 92.26%, respectively. The BUSCO analysis indicated that we captured a large
371 amount of conserved eukaryote and arthropod genes with 97.4% and 95.2% complete BUSCO
372 hits, respectively. Using the *D. melanogaster* proteome, the arthropod specific Uniprot/Swissprot
373 database and NCBI's non-redundant database of animal proteins, we successfully annotated
374 19,713 transcripts (32.2% of all transcripts) at a combined length of 32,039,513 bp (59% of the
375 full assembly). A total of 17,577 transcripts have a Gene Ontology (GO) annotation.

376 *Gene Ontology*

377 There were 179 scaffolds within 1 LOD of the QTL peaks combined. We mapped a total of
378 2,270 transcripts against 171 of the 179 scaffolds. We first tested whether QTL regions were
379 significantly enriched for genes involved in neurogenesis, ion channels, courtship behavior, and
380 neuromuscular development (Table S3). Testing the GO terms in the LOD1 intervals around the
381 QTL peaks across the 7 linkage groups with a significant QTL resulted in several enriched
382 biological processes. The ten most strongly enriched categories were related to locomotion

383 behavior, brain morphogenesis, metabolism, neuromuscular processes, and photoreceptor cell
384 specialization (Table S4, Fig S2). Among the other significantly (5% FDR) enriched categories
385 were calcium ion channel and ion transport regulation, peripheral nervous system development,
386 neuron differentiation, and neurotransmitter secretion, although these are just a few of the many
387 significantly enriched biological processes (Table S3). Testing each of the seven QTL region
388 separately, we found that all categories were enriched for several GO terms, including those
389 related to neuromuscular development (LG1, LG4), development, maintenance, and transmission
390 at synapses (LG1, LG3, LG5, LGX), rhythmic and locomotor behaviors (LG4, LG7), mating
391 behavior (LG3), hormone and pheromone production (LG2), and nervous system development
392 (LG4, LGX; Table S5).

393 **DISCUSSION**

394 Behavioral isolation is an important barrier to gene flow in the earliest stages of animal
395 speciation, but we know little about the number and distribution of underlying genetic loci and
396 their relationships with the tempo and mode of evolution. In island systems where founder
397 effects have been hypothesized in the history of species radiations, shifts in the phenotypic and
398 genetic environments due to genetic drift may enable speciation (Carson and Templeton 1984;
399 Templeton 2008), in particular for traits involved in sexual isolation (Van Oosterhout et al. 2003;
400 Templeton 2008; Bolund et al. 2010). In such a scenario, the genetic architecture has been
401 considered a lynch pin that can become reorganized upon disruption during the genetic upheaval
402 following the founder event. For this to occur, a type II genetic architecture (epistatic, major
403 gene/modifier) must underlie speciation phenotypes (Shaw and Mullen 2011; Mullen and Shaw
404 2014), such as those involved in sexual signaling. Conversely, it has been argued that a Type I
405 (additive, polygenic) genetic architecture, often underlies mating behavior divergence (Ritchie

406 and Phillips 1998). Here, we examine the genetic basis of interspecific variation in the song
407 rhythm between two swordtail cricket species that are isolated sexually (song and preference
408 behavior; Oh et al. 2012) and geographically (occupying different islands; Otte 1994; Mendelson
409 and Shaw 2005). We also provide compelling preliminary evidence that functional loci cluster in
410 specific regions associated with quantitative sexual traits and discuss some interesting homologs
411 of genes implicated in *Drosophila melanogaster* courtship behavior and in various
412 neurophysiological processes that can be tied to cricket song rhythm found within these regions.

413 *The genetic architecture of inter-island sexual trait divergence*

414 As opposed to documenting a contrast between the genetics of intra- versus inter-island
415 speciation events, we find significant parallels in QTL number, location, effect size, and
416 interaction between this study and an independently diverged intra-island species pair (Shaw et
417 al. 2007). We detected six moderate to small effect QTL for pulse rate variation on the seven
418 autosomes in *Laupala* and an additional small effect X-linked QTL. Based on our estimates of
419 the missing variation and number of undetected loci (Otto and Jones 2000), we conclude that the
420 true number of loci controlling pulse rate variation in *L. cerasina* and *L. eukolea* is likely more
421 than ten. Moreover, we found no detectable interaction effects among the identified QTL. Thus,
422 pulse rate divergence between these species most likely has a polygenic (Type I) genetic
423 architecture, rather than a Type II architecture, as has been hypothesized for speciation
424 phenotypes that interact with founder induced interisland speciation (Carson and Templeton
425 1984). These findings support earlier biometric evidence for both *L. kohalensis* by *L. paranigra*
426 and *L. cerasina* by *L. eukolea* species crosses (Shaw 1996; Oh et al. 2012). These results are
427 significant in that *Laupala* has one of the fastest rates of speciation known, yet a type I genetic
428 architecture underlies the interspecific genetics of an important speciation phenotype in this

429 radiation, independent of the biogeographic context. Other phenotypes may or may not follow
430 this pattern (e.g., Mullen et al. 2008) and merit further investigation.

431 Contrasting the results for *L. cerasina* and *L. eukolea* with those for *L. kohalensis* and *L.*
432 *paranigra* (Shaw et al. 2007) also uncovers that genetic differentiation in replicate *Laupala*
433 species pairs shows substantial parallelism. While the Shaw et al. (2007) study was based on
434 AFLP markers and the present study utilizes GBS markers, making precise comparisons of QTL
435 location challenging, some general comparisons between homologous linkage groups are
436 possible. Two major QTL on LG1 and LG3 explain around 12% and 8% of the average
437 phenotypic difference between *L. eukolea* and *L. cerasina*. The homologous linkage groups in
438 the genetic map of *L. kohalensis* and *L. paranigra* (linkage group numbers are the same, see also
439 Blankers et al. 2017 for linkage group homology) have QTL explaining around 9% and 10% of
440 the parental difference, respectively. Likewise, both the present study and *L. kohalensis* x *L.*
441 *paranigra* study find QTL effects on LG 4, LG5 and the X chromosome (the latter in line with
442 prior findings from biometric studies revealing a significant phenotypic difference in first
443 generation reciprocal hybrids (Shaw 1996; Oh et al. 2012)). Moreover, phenotype associations
444 on LG6 and LG7 were very weak or absent in both studies. Finally, all QTL allelic effects
445 estimated in this study and in Shaw et al. (2007) have directionality consistent with a hypothesis
446 of directional selection (Orr 1998; i.e., an allele originating from the fast (or slow) species
447 increases (or decreases) the pulse rate in hybrids).

448 There were also some differences between the two species pairs. While the QTL effects on LG4
449 and LG5 are present in both species pairs, they are larger in the *L. kohalensis* x *L. paranigra*
450 cross than in the current study (~0.14 and ~0.29 pps in the 2007 study, 0.05 and 0.07 pps in this
451 study). Additionally, we did not find evidence for secondary peaks on LG1 and LG3 (both had

452 small second peaks in the 2007 study) and detect only seven instead of eight QTL, despite
453 similar sample sizes and much denser genotype sampling (GBS SNP markers instead of AFLPs
454 used in the 2007 study). Estimates of the true number of loci also differs between the species
455 pairs, although both fit a polygenic architecture better than an oligogenic or major effect/epistasis
456 architecture (n = 14 (95% CI = [6-26]; at an estimated detection threshold of 0.025 pps) for this
457 study and n = 30 (95% CI = [15-55]; threshold = 0.040 pps) for Shaw et al. (2007), data from
458 table 2).

459 Together, our findings indicate that there is substantial genetic parallelism across species pairs,
460 that QTL on the same linkage groups largely have similar effect sizes, but that, by our estimates,
461 the number of causal loci differs. Morphological (Otte 1994) and molecular evidence
462 (Mendelson and Shaw 2005) place the two species pairs in independent species groups. Based on
463 records of island's geological history (Carson and Clague 1995), and the island endemism of *L.*
464 *kohalensis, L. paranigra* and *L. cerasina*, both species pairs have likely diverged in the last
465 500,000 years (Mendelson and Shaw 2005). Both groups show significant, conspicuous
466 differentiation in male and female sexual traits, but *L. kohalensis* and *L. paranigra* have diverged
467 to a greater degree (~ 3 pulses per second difference, versus ~ 1.6 pps for *L. eukolea* and *L.*
468 *cerasina*). Interestingly, this aligns well with the 2-fold difference in the estimated true number
469 of loci. Further comparative work is needed to probe the generality of these findings to better
470 illuminate the relationship between biogeography, magnitude of phenotypic divergence, and
471 genetic architecture of speciation.

472 As with any experiment, linkage mapping and QTL analyses are vulnerable to estimation error
473 (e.g., map order errors and false positive QTL) and an important way to mitigate this error, is
474 through replication. Here, we first studied the genetic architecture in two independent mapping

475 populations separately (mapping families HC1 and HC2), before combining the data to
476 maximize our sample size. The family-specific linkage maps are collinear, while the order was
477 determined independently for each map initially, providing support for the inferred marker order.
478 The major QTL on LG1 and LG3 have similar effect sizes and map to the same location in both
479 mapping populations. There are additional, smaller effect QTL that we detected in the larger
480 mapping population (HC2) only, likely a consequence of a larger sample size (similar to Shaw et
481 al. 2007). There are also QTL on LG2 and LG4 that were only detected after combining the two
482 mapping families. Thus, there is some corroboration of the results, which rules out
483 environmental sources of genotype-phenotype association and we also reveal some limitations to
484 detect small-effect QTL at lower sample sizes.

485 *Behavioral gene clusters*

486 Our results support the hypothesis that functionally related genes are clustered in specific
487 genomic regions. This is important because it suggests that QTL regions likely contain several
488 closely linked (and thus co-segregating) functionally related genes. Gene clusters reflect a
489 potential adaptation to overcome constraints associated with behavioral evolution that requires
490 coordinated change in several loci controlling complex neurophysiological traits. Close linkage
491 would reduce interspecific and intraspecific recombination and facilitate adaptation (Noor et al.
492 2001). It has been associated with several traits that are important in reproductive isolation
493 (Gould et al. 2010; Lowry and Willis 2010), speciation (Hermann et al. 2013), and mating
494 behavior variation (Küpper et al. 2015; Lamichhaney et al. 2015; Tuttle et al. 2016), specifically
495 in the light of trait-preference co-evolution (Lande 1981; Kirkpatrick 1982; Shaw et al. 2011;
496 Singh and Shaw 2012). In *Laupala* there is evidence for co-localization of male song and female
497 preference QTL (Shaw and Lesnick 2009; Wiley et al. 2012) and for male song QTL falling in

498 regions of low interspecific recombination, which might facilitate coordinated divergence among
499 genes underlying male song behavior and/or between male and female traits (Blankers et al.
500 2017). Additional fine-mapping approaches are necessary to see if any closely linked QTL can
501 be detected once more recombination events can be observed (at higher sample sizes).

502 Our results also shed light on the potential genetic mechanisms that control mating behavior
503 variation in *Laupala*. The main enriched biological processes among the predicted gene products
504 in QTL regions can be tied to potential modulators of central pattern generators (rhythmic
505 behaviors) and to sex-specific expression in nervous system development pathways in fruit flies:
506 various neuromuscular processes, nervous system development, neurotransmitter secretion, and
507 other neurological processes. These findings were in part driven by potential homologs of *lola* (6
508 cM away from the peak at LG4), *semaphorin* (directly flanking the peak at LG7), and
509 *roundabout* (1.5 cM away from the peak at LG1). All three of these genes are affected by sex-
510 specific transcription of *fruitless* (which itself is located on LG2) in *D. melanogaster* and
511 contribute to sexual dimorphism in the nervous system (Moran and Kyriacou 2009; Dauwalder
512 2011; Nojima et al. 2014).

513 In addition to these sex specific receptor proteins, we find receptors for serotonin, GABA,
514 dopamine, and acetylcholine, all known neuromodulators of central pattern generators in insects
515 (Marder and Bucher 2001; Gerhardt and Huber 2002; Katz 2016). We also identify several ion
516 channel genes such as *cadherin* (flanking the QTL peak marker on LG3), *cacophony* (16 cM
517 from the peak on LG4, which has a functional role in the inter-pulse interval in *D. melanogaster*
518 Peixoto and Hall 1998), *KCNQ potassium channel* (1.5 cM from peak marker on LG3), and
519 *sandman* (1.9 cM from the peak at LG5). We acknowledge that without functional genetic
520 experiments (e.g. knockout experiments) and tissue specific expression screens (to check if

521 expression of these genes is sex-specific and/or if they are active in the mesothorax where the
522 central pattern generators are located) there is no conclusive evidence that these genes are
523 involved in modulation of the central pattern generator or song rhythm in *Laupala*. Overall,
524 however, QTL regions are significantly enriched for a variety of processes related to
525 neuromodulation and nervous system development and multiple QTL harbor interesting
526 candidate loci for central pattern generator modulation and courtship behavior, which merit
527 follow-up analyses and functional validation.

528 Together, this study presents rare comparative insights into the polygenic genetic architecture
529 associated with sexual trait divergence during speciation in different biogeographic contexts.
530 Clearly, rapid quantitative trait differentiation associated with speciation can occur under a Type
531 I genetic architecture, where many genes diverge in concert to produce a conspicuous species
532 difference. We show that the genetic architecture of male song rhythm divergence in closely
533 related *Laupala* species is remarkably similar among two independently originated species pairs,
534 despite their different geographic histories. Through this study, we further identify several
535 potential candidate genes controlling this highly divergent and isolating behavioral phenotype.
536 We show that the QTL regions underlying song pulse rate divergence identified in this study are
537 enriched for a variety of neuromuscular processes that may contribute to modulating the central
538 pattern generators that control the song rhythm. This finding suggests potential clustering of
539 functionally related loci in small genomic regions, which warrant additional research.

540

541

542 **REFERENCES**

543 Alexa, A., and J. Rahnenfuhrer. 2016. topGO: Enrichment Analysis for Gene Ontology.

544 Alexander, R. 1962. Evolutionary change in cricket acoustical communication. Evolution.
545 16:443–467.

546 Altschul, S. F., W. Gish, W. Miller, E. W. Myers, and D. J. Lipman. 1990. Basic local alignment
547 search tool. J. Mol. Biol. 215:403–410.

548 Aronesty, E. 2011. ea-utils: Command-line tools for processing biological sequencing data. Expr.
549 Anal. Durham, NC.

550 Benjamini, Y., and Y. Hochberg. 1995. Controlling the false discovery rate: a practical and
551 powerful approach to multiple testing. J. R. Stat. Soc. Ser. B 289–300.

552 Blankers, T., K. P. Oh, A. Bombarely, and K. L. Shaw. 2017. The genomic architecture of a
553 rapid island radiation: mapping chromosomal rearrangements and recombination rate
554 variation in Laupala. bioRxiv, doi: 10.1101/160952.

555 Boake, C. R. B. C. R. B., S. J. S. J. Arnold, F. Breden, L. M. L. M. Meffert, M. G. M. G. Ritchie,
556 B. J. B. J. Taylor, J. B. J. B. Wolf, and a. J. A. J. Moore. 2002. Genetic tools for studying
557 adaptation and the evolution of behavior. Am. Nat. 160 Suppl:S143–S159.

558 Bolund, E., K. Martin, B. Kempenaers, and W. Forstmeier. 2010. Inbreeding depression of
559 sexually selected traits and attractiveness in the zebra finch. Anim. Behav. 79:947–955.

560 Broman, K. W., H. Wu, Ś. Sen, and G. A. Churchill. 2003. R/qtl: QTL mapping in experimental
561 crosses. Bioinformatics 19:889–890.

562 Camacho, C., G. Coulouris, V. Avagyan, N. Ma, J. Papadopoulos, K. Bealer, and T. L. Madden.

563 2009. BLAST+: architecture and applications. BMC Bioinformatics 10:421.

564 Cande, J., D. L. Stern, T. Morita, B. Prud'homme, and N. Gompel. 2014. Looking Under the
565 Lamp Post: Neither fruitless nor doublesex Has Evolved to Generate Divergent Male
566 Courtship in Drosophila. Cell Rep. 8:363–370.

567 Carson, H. L., and D. A. Clague. 1995. Hawaiian Biogeography: Evolution on a Hot Spot
568 Archipelago. Smithsonian Institution Press, Washington, DC.

569 Carson, H. L., and A. R. Templeton. 1984. Genetic revolutions in relation to speciation
570 phenomena: the founding of new populations. Annu. Rev. Ecol. Syst. 15:97–132.

571 Chenoweth, S. F., and K. McGuigan. 2010. The Genetic Basis of Sexually Selected Variation.
572 Annu. Rev. Ecol. Evol. Syst. 41:91–101.

573 Clyne, J. D., and G. Miesenböck. 2008. Sex-Specific Control and Tuning of the Pattern
574 Generator for Courtship Song in Drosophila. Cell 133:354–363.

575 Conesa, A., S. Götz, J. M. García-Gómez, J. Terol, M. Talón, and M. Robles. 2005. Blast2GO: A
576 universal tool for annotation, visualization and analysis in functional genomics research.
577 Bioinformatics 21:3674–3676.

578 Coyne, J. A., and H. A. Orr. 2004. Speciation. Sinauer, Sunderland, MA.

579 Crocker, A., M. Shahidullah, I. B. Levitan, and A. Sehgal. 2010. Identification of a neural circuit
580 that underlies the effects of octopamine on sleep: wake behavior. Neuron 65:670–681.

581 Danecek, P., A. Auton, G. Abecasis, C. A. Albers, E. Banks, M. A. DePristo, R. E. Handsaker,
582 G. Lunter, G. T. Marth, S. T. Sherry, G. McVean, R. Durbin, and 1000 Genomes Project
583 Analysis Group. 2011. The variant call format and VCFtools. Bioinforma. 27:2156–2158.

584 Dauwalder, B. 2011. The roles of fruitless and doublesex in the control of male courtship. Int
585 Rev Neurobiol 99:87–105.

586 Dawkins, R. 1976. The Selfish Gene. Oxford Univ Press, Oxford.

587 de Goor, T. A. 2003. The principle and promise of labchip technology. Pharma Genomics 3:16–
588 18.

589 DePristo, M. A., E. Banks, R. Poplin, K. V Garimella, J. R. Maguire, C. Hartl, A. A. Philippakis,
590 G. del Angel, M. A. Rivas, M. Hanna, A. McKenna, T. J. Fennell, A. M. Kernytsky, A. Y.
591 Sivachenko, K. Cibulskis, S. B. Gabriel, D. Altshuler, and M. J. Daly. 2011. A framework
592 for variation discovery and genotyping using next-generation DNA sequencing data. Nat.
593 Genet. 43:491–498.

594 Dieckmann, U., and M. O. Doebeli. 1999. On the origin of species by sympatric speciation.
595 Nature 400:354–357.

596 Dodt, M., J. T. Roehr, R. Ahmed, and C. Dieterich. 2012. FLEXBAR—flexible barcode and
597 adapter processing for next-generation sequencing platforms. Biology. 1:895–905.

598 Doorn, G. van, P. Edelaar, and F. Weissing. 2009. On the origin of species by natural and sexual
599 selection. Science 326:1704–1707.

600 Elshire, R. J., J. C. Glaubitz, Q. Sun, J. A. Poland, K. Kawamoto, and E. S. Buckler. 2011. A
601 robust, simple genotyping-by-sequencing (GBS) approach for high diversity species. PLoS
602 One. 6.

603 Endelman, J. B., and C. Plomion. 2014. LPmerge: an R package for merging genetic maps by
604 linear programming. Bioinformatics 30:1623–1624.

605 Etges, W. J., C. C. De Oliveira, E. Gragg, D. Ortiz-Barrientos, M. A. F. Noor, and M. G. Ritchie.
606 2007. Genetics of incipient speciation in Drosophila mojavensis. I. Male courtship song,
607 mating success, and genotype x environment interactions. Evolution. 61:1106–1119.

608 Fisher, R. 1930. The genetical theory of natural selection. Oxford University Press, New York.

609 Fishman, L., A. J. Kelly, and J. H. Willis. 2002. Minor quantitative trait loci underlie floral traits
610 associated with mating system divergence in Mimulus. Evolution; 56:2138–2155.

611 Garrison, E., and G. Marth. 2012. Haplotype-based variant detection from short-read sequencing.
612 arXiv Prepr. arXiv1207.3907.

613 Gerhardt, H. C., and F. Huber. 2002. Acoustic communication in insects and anurans. The
614 University of Chicago Press, Chicago.

615 Gleason, J. M. 2005. Mutations and natural genetic variation in the courtship song of Drosophila.
616 Behav. Genet. 35:265–277.

617 Gould, F., M. Estock, N. K. Hillier, B. Powell, A. T. Groot, C. M. Ward, J. L. Emerson, C.
618 Schal, and N. J. Vickers. 2010. Sexual isolation of male moths explained by a single
619 pheromone response QTL containing four receptor genes. Proc. Natl. Acad. Sci. U. S. A.
620 107:8660–8665.

621 Gourbiere, S. 2004. How do natural and sexual selection contribute to sympatric speciation ? J.
622 Evol. Biol. 17:1297–1309.

623 Grace, J. L., and K. L. Shaw. 2011. Coevolution of male mating signal and female preference
624 during early lineage divergence of the Hawaiian cricket, Laupala Cerasina. Evolution.
625 65:2184–2196.

626 Gramates, L. S., S. J. Marygold, G. dos Santos, J.-M. Urbano, G. Antonazzo, B. B. Matthews, A.
627 J. Rey, C. J. Tabone, M. A. Crosby, D. B. Emmert, K. Falls, J. L. Goodman, Y. Hu, L.
628 Ponting, A. J. Schroeder, V. B. Strelets, J. Thurmond, and P. Zhou. 2017. FlyBase at 25:
629 looking to the future. Nucleic Acids Res. 45:D663–D671.

630 Grossmann, S., S. Bauer, P. N. Robinson, and M. Vingron. 2007. Improved detection of
631 overrepresentation of Gene-Ontology annotations with parent--child analysis.
632 Bioinformatics 23:3024–3031.

633 Haas, B. J., A. Papanicolaou, M. Yassour, M. Grabherr, P. D. Blood, J. Bowden, M. B. Couger,
634 D. Eccles, B. Li, M. Lieber, M. D. MacManes, M. Ott, J. Orvis, N. Pochet, F. Strozzi, N.
635 Weeks, R. Westerman, T. William, C. N. Dewey, R. Henschel, R. D. LeDuc, N. Friedman,
636 and A. Regev. 2013. De novo transcript sequence reconstruction from RNA-seq using the
637 Trinity platform for reference generation and analysis. Nat. Protoc. 8:1494–1512.

638 Haley, C. S., and S. A. Knott. 1992. A simple regression method for mapping quantitative trait
639 loci in line crosses using flanking markers. Heredity. 69:315–324.

640 Harrison, R. G. 1991. Molecular changes at speciation. Annu. Rev. Ecol. Syst. 22:281–308.

641 Hedwig, B. 2014. Towards an Understanding of the Neural Basis of Acoustic Communication in
642 Crickets. Pp. 123–141 *in* B. Hedwig, ed. Insect Hearing and Acoustic Communication.
643 Springer, Berlin.

644 Hennig, R. M., and D. Otto. 1996. No Title. Zoology 99:268–276.

645 Hermann, K., U. Klahre, M. Moser, H. Sheehan, T. Mandel, and C. Kuhlemeier. 2013. Tight
646 genetic linkage of prezygotic barrier loci creates a multifunctional speciation island in

647 Petunia. Curr. Biol. 23:873–877.

648 Hoekstra, H. E. 2010. In search of the elusive behavior gene. Search Causes Evol. From F. Obs.
649 to Mech. 192–210. Princeton University Press New Jersey, NJ.

650 Jones, P., D. Binns, H.-Y. Chang, M. Fraser, W. Li, C. McAnulla, H. McWilliam, J. Maslen, A.
651 Mitchell, G. Nuka, and others. 2014. InterProScan 5: genome-scale protein function
652 classification. Bioinformatics 30:1236–1240.

653 Katz, P. S. 2016. Evolution of central pattern generators and rhythmic behaviours. Philos. Trans.
654 R. Soc. B Biol. Sci. 371:20150057.

655 Kent, W. J. 2002. BLAT—the BLAST-like alignment tool. Genome Res. 12:656–664.

656 Kim, D., B. Langmead, and S. L. Salzberg. 2015. HISAT: a fast spliced aligner with low
657 memory requirements. Nat. Methods 12:357–360.

658 Kirkpatrick, M., and V. Ravigne. 2002. Speciation by natural and sexual selection: models and
659 experiments. Am. Nat. 159 supple:S22–S35.

660 Kirkpatrick, P. 1982. Sexual selection and the evolution of female mate choice.

661 Küpper, C., M. Stocks, J. E. Risse, N. Remedios, L. L. Farrell, B. Mcrae, T. C. Morgan, N.
662 Karlionova, P. Pinchuk, Y. I. Verkuil, A. S. Kitaysky, J. C. Wingfield, T. Piersma, K. Zeng,
663 J. Slate, M. Blaxter, D. B. Lank, and T. Burke. 2015. A supergene determines highly
664 divergent male reproductive morphs in the ruff. Nat. Gen. 48:79–83.

665 Lamichhaney, S., G. Fan, F. Widemo, U. Gunnarsson, D. S. Thalmann, M. P. Hoeppner, S.
666 Kerje, U. Gustafson, C. Shi, H. Zhang, W. Chen, X. Liang, L. Huang, J. Wang, E. Liang, Q.
667 Wu, S. M.-Y. Lee, X. Xu, J. Höglund, X. Liu, and L. Andersson. 2015. Structural genomic

668 changes underlie alternative reproductive strategies in the ruff (Philomachus pugnax). Nat.
669 Genet. 48:84–88.

670 Lande, R. 1981. Models of speciation by sexual selection on polygenic traits. Proc Natl Acad Sci
671 U S A 78:3721–3725.

672 Lander, E., P. Green, J. Abrahamson, A. Barlow, M. Daly, S. Lincoln, and L. Newburg. 1987.
673 MAPMAKER: An interactive computer package for constructing primary genetic linkage
674 maps of experimental and natural populations. Genomics 1:174–181.

675 Langmead, B., and S. L. Salzberg. 2012. Fast gapped-read alignment with Bowtie 2. Nat.
676 Methods 9:357–359.

677 Li, H., B. Handsaker, A. Wysoker, T. Fennell, J. Ruan, N. Homer, G. Marth, G. Abecasis, and R.
678 Durbin. 2009. The sequence alignment/map format and SAMtools. Bioinformatics
679 25:2078–2079.

680 Liu, Y., J. Schröder, and B. Schmidt. 2013. Musket: a multistage k-mer spectrum-based error
681 corrector for Illumina sequence data. Bioinformatics 29:308–315. Oxford Univ Press.

682 Lowry, D. B., and J. H. Willis. 2010. A widespread chromosomal inversion polymorphism
683 contributes to a major life-history transition, local adaptation, and reproductive isolation.
684 PLoS Biol. 8:e1000500.

685 Mackay, T. F. C. 2001. The genetic architecture of quantitative traits. Annu. Rev. Genet.
686 35:303–339.

687 Marder, E., and D. Bucher. 2001. Central pattern generators and the control of rythmic
688 movements. Curr. Biol. 11:R986–R996.

689 Mayr, E. 1963. Animal Species and Evolution. Harvard University Press.

690 Mendelson, T. C., and K. L. Shaw. 2005. Rapid speciation in an arthropod. Nature 433:375–376.

691 Mendelson, T. C., A. M. Siegel, and K. L. Shaw. 2004. Testing geographical pathways of
692 speciation in a recent island radiation. Mol. Ecol. 13:3787–3796.

693 Mittleman, B. E., B. Manzano-Winkler, J. B. Hall, K. L. Korunes, and M. A. F. Noor. 2017. The
694 large X-effect on secondary sexual characters and the genetics of variation in sex comb
695 tooth number in Drosophila subobscura . Ecol. Evol. 7:533–540.

696 Moran, C. N., and C. P. Kyriacou. 2009. Functional neurogenomics of the courtship song of
697 male Drosophila melanogaster. Cortex 45:18–34.

698 Mullen, S. P., J. G. Millar, C. Schal, and K. L. Shaw. 2008. Identification and characterization of
699 cuticular hydrocarbons from a rapid species radiation of Hawaiian swordtailed crickets
700 (Gryllidae: Trigonidiinae: Laupala). J. Chem. Ecol. 34:198–204.

701 Mullen, S. P., and K. L. Shaw. 2014. Insect speciation rules: unifying concepts in speciation
702 research. Annu. Rev. Entomol. 59:339–361.

703 Nojima, T., M. C. Neville, and S. F. Goodwin. 2014. Fruitless isoforms and target genes specify
704 the sexually dimorphic nervous system underlying Drosophila reproductive behavior. Fly
705 (Austin). 8:95–100.

706 Noor, M. A. F., A. L. Cunningham, and J. C. Larkin. 2001. Consequences of recombination rate
707 variation on quantitative trait locus mapping studies: simulations based on the Drosophila
708 melanogaster genome. Genetics 159:581–588.

709 Oh, K. P., D. J. Fergus, J. L. Grace, and K. L. Shaw. 2012. Interspecific genetics of speciation

710 phenotypes: Song and preference coevolution in Hawaiian crickets. J. Evol. Biol. 25:1500–
711 1512.

712 Oh, K. P., and K. L. Shaw. 2013. Multivariate sexual selection in a rapidly evolving speciation
713 phenotype. Proc. Biol. Sci. 280:20130482.

714 Orr, H. A. 1998. Testing natural selection vs. genetic drift in phenotypic evolution using
715 quantitative trait locus data. Genetics 149:2099–2104.

716 Otte, D. 1992. Evolution of cricket songs. J. Orthoptera Res. 1:25–49.

717 Otte, D. 1994. The Crickets of Hawaii: Origin, Systematics, and Evolution. Orthoptera
718 Society/Academy of Natural Sciences of Philadelphia, Philadelphia, PA.

719 Otto, S. P., and C. D. Jones. 2000. Detecting the undetected: Estimating the total number of loci
720 underlying a quantitative trait. Genetics 156:2093–2107.

721 Peixoto, A. A., and J. C. Hall. 1998. Analysis of temperature-sensitive mutants reveals new
722 genes involved in the courtship song of Drosophila. Genetics 148:827–838.

723 Qvarnström, A., and R. I. Bailey. 2009. Speciation through evolution of sex-linked genes.
724 Heredity. 102:4–15.

725 Ritchie, M. G., and S. D. F. Phillips. 1998. The genetics of sexual isolation. P. 291 *in* D. J.
726 Howard and S. H. Berlocher, eds. Endless Forms: Species and Speciation. Oxford
727 University Press, New York.

728 Schmieder, R., and R. Edwards. 2011. Quality control and preprocessing of metagenomic
729 datasets. Bioinformatics 27:863–864.

730 Schöneich, S., and B. Hedwig. 2017. Neurons and Networks Underlying Singing Behaviour. Pp.

141–153 *in* H. W. Horch, T. Mito, A. Popadić, H. Ohuchi, and S. Noji, eds. The Cricket as a Model Organism: Development, Regeneration, and Behavior. Springer Japan, Tokyo.

Schwander, T., R. Libbrecht, and L. Keller. 2014. Supergenes and Complex Phenotypes. Curr. Biol. 24:R288–R294.

Sen, Ś., and G. A. Churchill. 2001. A statistical framework for quantitative trait mapping. Genetics 159:371–387.

Servedio, M. R., and R. Burger. 2014. The counterintuitive role of sexual selection in species maintenance and speciation. Proc. Natl. Acad. Sci. 111:8113–8118.

Shaw, K. L. 2000. Interspecific genetics of mate recognition: inheritance of female acoustic preference in Hawaiian crickets. Evolution 54:1303–1312.

Shaw, K. L. 1996. Polygenic Inheritance of a Behavioral Phenotype: Interspecific Genetics of Song in the Hawaiian Cricket Genus Laupala. Evolution. 50:256–266.

Shaw, K. L., C. K. Ellison, K. P. Oh, and C. Wiley. 2011. Pleiotropy, “sexy” traits, and speciation. Behav. Ecol. 22:1154–1155.

Shaw, K. L., and S. C. Lesnick. 2009. Genomic linkage of male song and female acoustic preference QTL underlying a rapid species radiation. Proc. Natl. Acad. Sci. U. S. A. 106:9737–9742.

Shaw, K. L., and S. P. Mullen. 2011. Genes versus phenotypes in the study of speciation. Genetica 139:649–661.

Shaw, K. L., and Y. M. Parsons. 2002. Divergence of mate recognition behavior and its consequences for genetic architectures of speciation. Am. Nat. 159 Suppl:S61–S75.

752 Shaw, K. L., Y. M. Parsons, and S. C. Lesnick. 2007. QTL analysis of a rapidly evolving
753 speciation phenotype in the Hawaiian cricket Laupala. Mol. Ecol. 16:2879–2892.

754 Simão, F. A., R. M. Waterhouse, P. Ioannidis, E. V Kriventseva, and E. M. Zdobnov. 2015.
755 BUSCO: assessing genome assembly and annotation completeness with single-copy
756 orthologs. Bioinformatics 31:3210.

757 Singh, N. D., and K. L. Shaw. 2012. On the scent of pleiotropy. Proc. Natl. Acad. Sci. 109:5–6.

758 Templeton, A. R. 1981. Mechanisms of speciation--A popularion genetic approach. Annu. Rev.
759 Ecol. Syst. 12:23–48.

760 Templeton, A. R. 2008. The reality and importance of founder speciation in evolution. BioEssays
761 30:470–479.

762 The UniProt Consortium. 2017. UniProt: the universal protein knowledgebase. Nucleic Acids
763 Res. 45:D158--D169.

764 Tuttle, E. M., A. O. Bergland, M. L. Korody, M. S. Brewer, D. J. Newhouse, P. Minx, M. Stager,
765 A. Betuel, Z. A. Cheviron, W. C. Warren, and others. 2016. Divergence and functional
766 degradation of a sex chromosome-like supergene. Curr. Biol. 26:344–350.

767 Van der Auwera, G. A., M. O. Carneiro, C. Hartl, R. Poplin, G. del Angel, A. Levy-Moonshine,
768 T. Jordan, K. Shakir, D. Roazen, J. Thibault, E. Banks, K. V Garimella, D. Altshuler, S.
769 Gabriel, and M. A. DePristo. 2013. From FastQ Data to High-Confidence Variant Calls:
770 The Genome Analysis Toolkit Best Practices Pipeline. Curr. Protoc. Bioinforma. 43:1–11.

771 Van Oosterhout, C., R. E. Trigg, G. R. Carvalho, A. E. Magurran, L. Hauser, and P. W. Shaw.
772 2003. Inbreeding depression and genetic load of sexually selected traits: how the guppy lost

773 its spots. J. Evol. Biol. 16:273–281.

774 Veltsos, P., E. Gregson, B. Morrissey, J. Slate, A. Hoikkala, R. K. Butlin, and M. G. Ritchie.
775 2015. The genetic architecture of sexually selected traits in two natural populations of
776 Drosophila montana. Heredity. 115:565.

777 West-Eberhard, M. J. 1983. Sexual selection, social competition, and speciation. Q. Rev. Biol.
778 58:155–183.

779 Wiley, C., C. Ellison, and K. Shaw. 2012. Widespread genetic linkage of mating signals and
780 preferences in the Hawaiian cricket Laupala. Proc. R. Soc. B Biol. Sci. 279:1203–1209.

781 Wu, T. D., and C. K. Watanabe. 2005. GMAP: a genomic mapping and alignment program for
782 mRNA and EST sequences. Bioinformatics 21:1859–1875.

783 Yamamoto, D., and M. Koganezawa. 2013. Genes and circuits of courtship behaviour in
784 Drosophila males. Nat. Rev. Neurosci. 14:681–92.

785 Zdobnov, E. M., and R. Apweiler. 2001. InterProScan--an integration platform for the signature-
786 recognition methods in InterPro. Bioinformatics 17:847–848.

787

788

789 **TABLES**

790 Table 1. Phenotypic distributions. The mean, standard deviation, and sample size of the pulse rate (pulses per
791 second) are shown for the parental species and the F2 generation (both cross types, HC1 and HC2).

	Mean (pps)	**sd**	**n**
L. cerasina	2.33	0.07	24
L. eukolea	3.99	0.12	16
Environmental Variance*	0.02	0.13	
F2 HC1	3.11	0.20	94
F2 HC2	3.16	0.23	136
F2 mean	3.14	0.22	230

792 *Environmental variance was calculate following (Fishman et al. 2002); "mean" in this context refers to the
793 environmental variance, while "sd" is the square root of that variance.

794

795 Table 2. QTL results from HC1 and HC2. QTL were mapped using the maps for the 94 HC1 and 136 HC2 F2
796 individuals. LOD: log-of-odds. A and B alleles denote *L. cerasina* and *L. eukolea* alleles, respectively. All QTL
797 effects are significantly different from zero (* P < 0.05; † P < 0.01; ‡ P < 0.001). ESD: environmental standard
798 deviation.

					Phenotypic Value						
Linkage group	QTL location (cM)	LOD	Nearest scaffold	Marker location	AA	AB	BB	QTL effect (pps +/- SD)	QTL effect (% parental difference)	QTL effect (#ESDs)	% F2 variance explained
HC1											
1	119	17.81	S004794	119.4	2.88	3.14	3.31	0.220 +/- 0.021†	13.23	1.75	50.60
3	71.3	7.04	S001552	71.3	2.95	3.13	3.16	0.116 +/- 0.020‡	6.95	0.92	14.96
HC2											
1	57.0	23.85	S002490	56.9	2.90	3.18	3.31	0.216 +/- 0.017†	13.03	1.72	37.05
3	67.1	12.98	S000355	67.1	3.03	3.17	3.28	0.136 +/- 0.016†	8.18	1.08	16.46
5	48.9	5.38	S001294	48.9	3.04	3.17	3.25	0.076 +/- 0.015*	4.55	0.60	5.96
7	56.0	2.63	S001482	56.1	3.10	3.14	3.29	0.056 +/- 0.017*	3.38	0.44	2.78
X	32.0	3.74	S000108	29.7	3.13	3.19	3.13	0.049 +/- 0.012*	2.93	0.39	4.03

799

800

801 Table 3. QTL results from the combined map. QTL were mapped using the consensus map for the 230 F2
802 individuals. LOD: log-of-odds. A and B alleles denote *L. cerasina* and *L. eukolea* alleles, respectively. All QTL
803 effects are significantly different from zero (* P < 0.05; † P < 0.01; ‡ P < 0.001). ESD: environmental standard
804 deviation.

					Phenotypic value						
Linkage group	QTL location (cM)	LOD	Nearest scaffold	Marker location	AA	AB	BB	QTL effect (pps +/- SD)	QTL effect (% parental difference)	QTL effect (#ESDs)	% F2 variance explained
1	59.0	40.73	S001131	58.8	2.89	3.17	3.31	0.203 +/- 0.013	12.25	1.61	36.39
2	71.0	4.78	S001921	69.1	3.05	3.15	3.18	0.055 +/- 0.013	3.31	0.44	2.90
3	79.9	21.28	S000385	79.9	3.02	3.14	3.23	0.123 +/- 0.012	7.42	0.98	15.34
4	59.8	3.97	S016452	59.0	3.10	3.12	3.23	0.053 +/- 0.013	3.20	0.42	2.39
5	36.9	8.32	S002445	36.9	3.05	3.16	3.19	0.068 +/- 0.012	4.09	0.54	5.23
7	5.0	3.51	S007011	9.8	3.08	3.14	3.20	0.045 +/- 0.013	2.69	0.35	2.10
X	38.0	5.46	S003132	37.2	3.10	3.17	3.10	0.041 +/- 0.009	2.46	0.32	3.34
cross	-	2.24	-	-	-	-	-	0.055 +/- 0.018	3.31	0.44	1.33

805
806

807 **FIGURE LEGENDS**

808 Figure 1. Phenotypic distributions for the parental lines and first and second-generation hybrid
809 offspring. The data from the F1 hybrids in the top panel are from Oh et al. 2012 and shown to
810 illustrate F1 distributions as well as the maternal bias in pulse rate inheritance. The F2 data are
811 split by family/mapping population (HC1 and HC2).

812 Figure 2. Results from the multiple QTL models (black solid lines, only for linkage groups with
813 significant QTL) and composite interval mapping (grey solid lines). The vertical dotted line
814 shows the 5% significance threshold for the composite interval mapping. The horizontal dotted
815 lines connect homologous markers nearby QTL peaks in HC1 and HC2 to illustrate the overlap
816 between the QTL scans in the different mapping populations. The panels on the far right show
817 the effect size of each of the QTL as the pulse rate mean +/- standard error for each of the
818 genotype categories AA (left), AB (center), BB (right).

819 Figure S1. Linkage map and multivariate QTL model results. The horizontal black bars show the
820 position of the SNP markers in the HC1, combined, and HC2 map, respectively. The black dots
821 and solid lines connect homologous scaffolds between adjacent linkage groups. The scale
822 indicates the position along the linkage group in cM. The red vertical bars and error bars show
823 the 1-LOD and 2-LOD interval around the QTL peaks, respectively. QTL were calculated using
824 a multivariate model and significance was inferred using penalized LOD scores.

825 Figure S2. Enriched Gene Ontology network. The 10 most strongly enriched biological processes
826 (squares) and their relationship (arrows) as well as associated parental terms (ellipses) are shown.
827 The colors correlate with the parent-child algorithm corrected *P* values (not with FDR corrected
828 q-values). Warmer colors (more red) indicate lower *P* values.

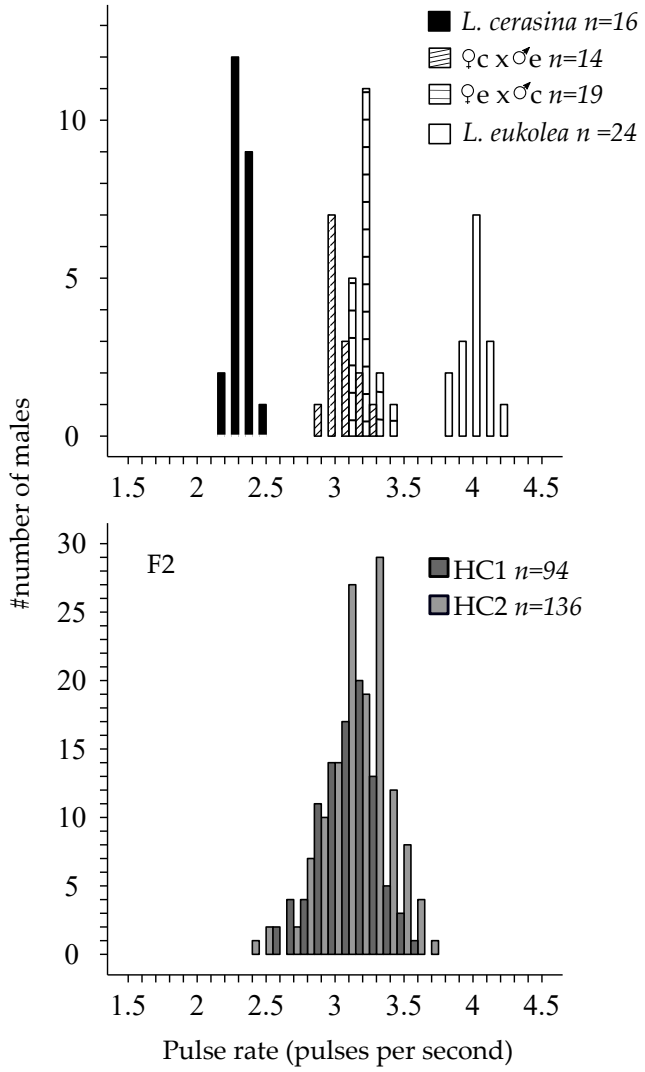

Figure 1. Phenotypic distributions for the parental lines and first and second-generation hybrid offspring. The data from the F1 hybrids in the top panel is from Oh et al. 2012 and shown to illustrate F1 distributions as well as the maternal bias in pulse rate inheritance. The F2 data is split by family/mapping population (HC1 and HC2).

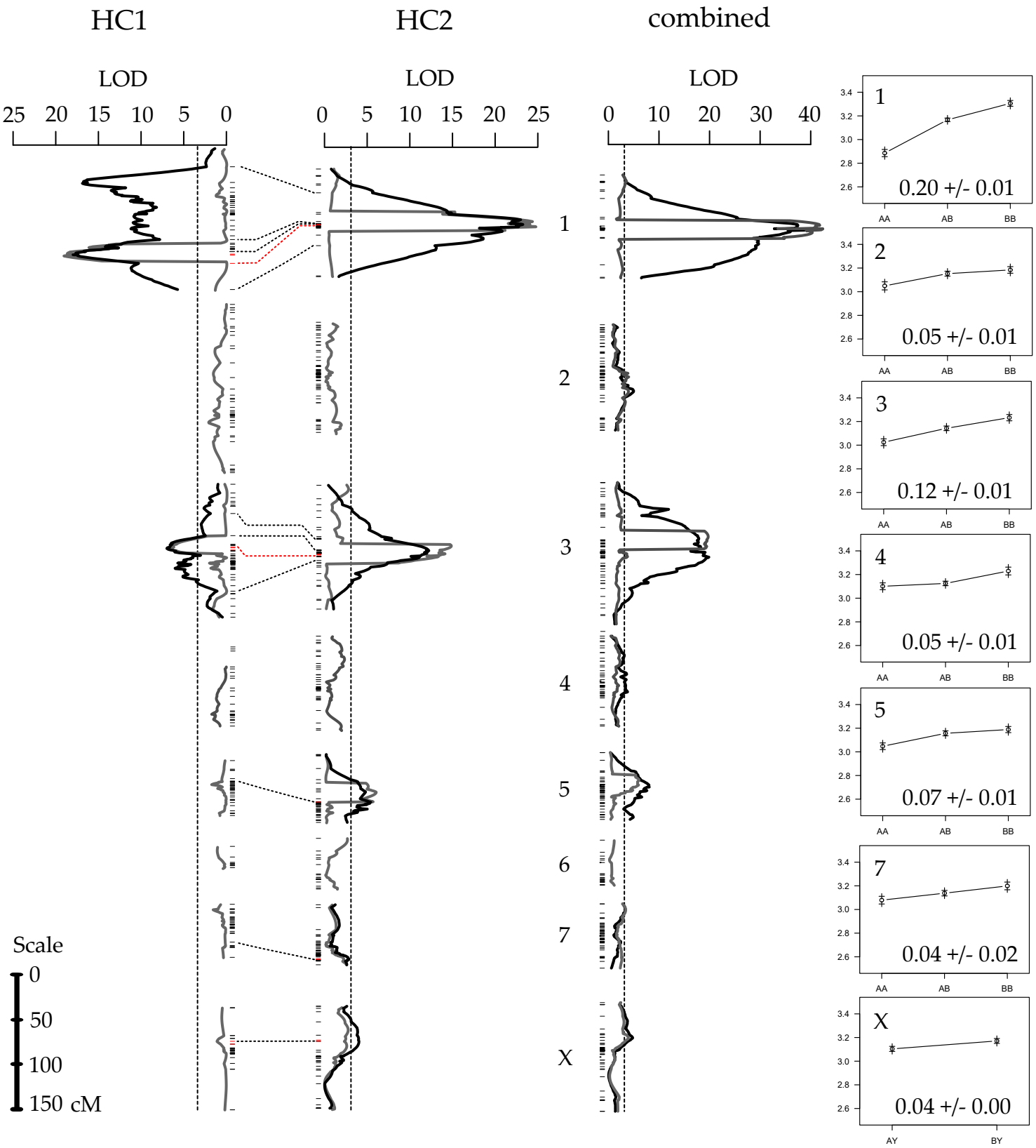

Figure 2. Results from the multiple QTL models (black solid lines, only for linkage groups with significant QTL) and composite interval mapping (grey solid lines). The vertical dotted line shows the 5% significance threshold for the composite interval mapping. The horizontal dotted lines connect homologous markers nearby QTL peaks in HC1 and HC2 to illustrate the overlap between the QTL scans in the different mapping populations. The panels on the far right show the effect size of each of the QTL as the pulse rate mean+/-standard error for each of the genotype categories AA, AB, BB.

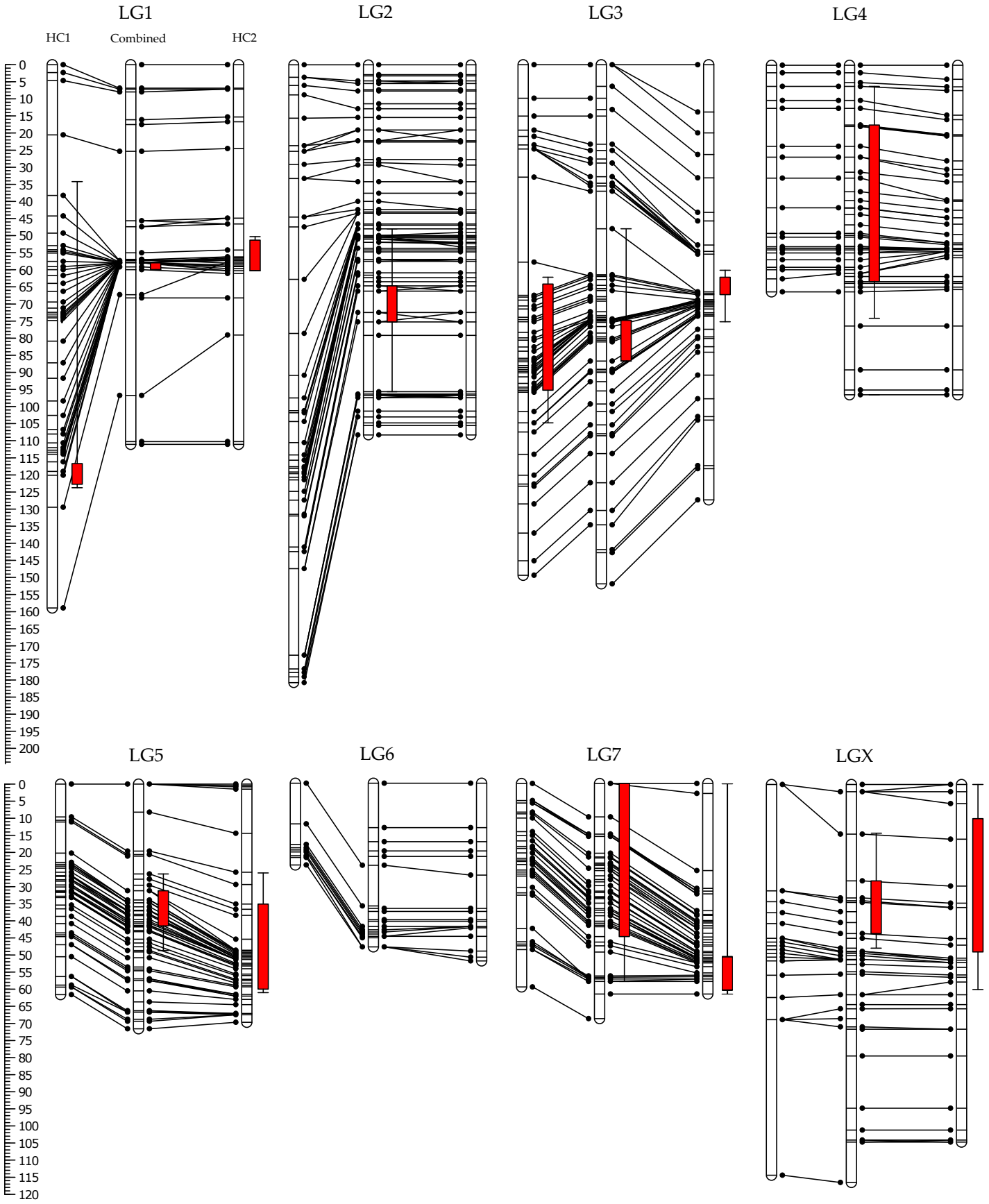

Figure S1. Linkage map and multivariate QTL model results. The horizontal black bars show the position of the SNP markers in the HC1, combined, and HC2 map, respectively. The black dots and solid lines connect homologous scaffolds between adjacent linkage groups.The scale indicates the position along the linkage group in cM. The red vertical bars and error bars show the 1-LOD and 2-LOD interval around the QTL peaks, respectively. QTL were calculated using a multivariate model and significance was inferred using penalized LOD scores.

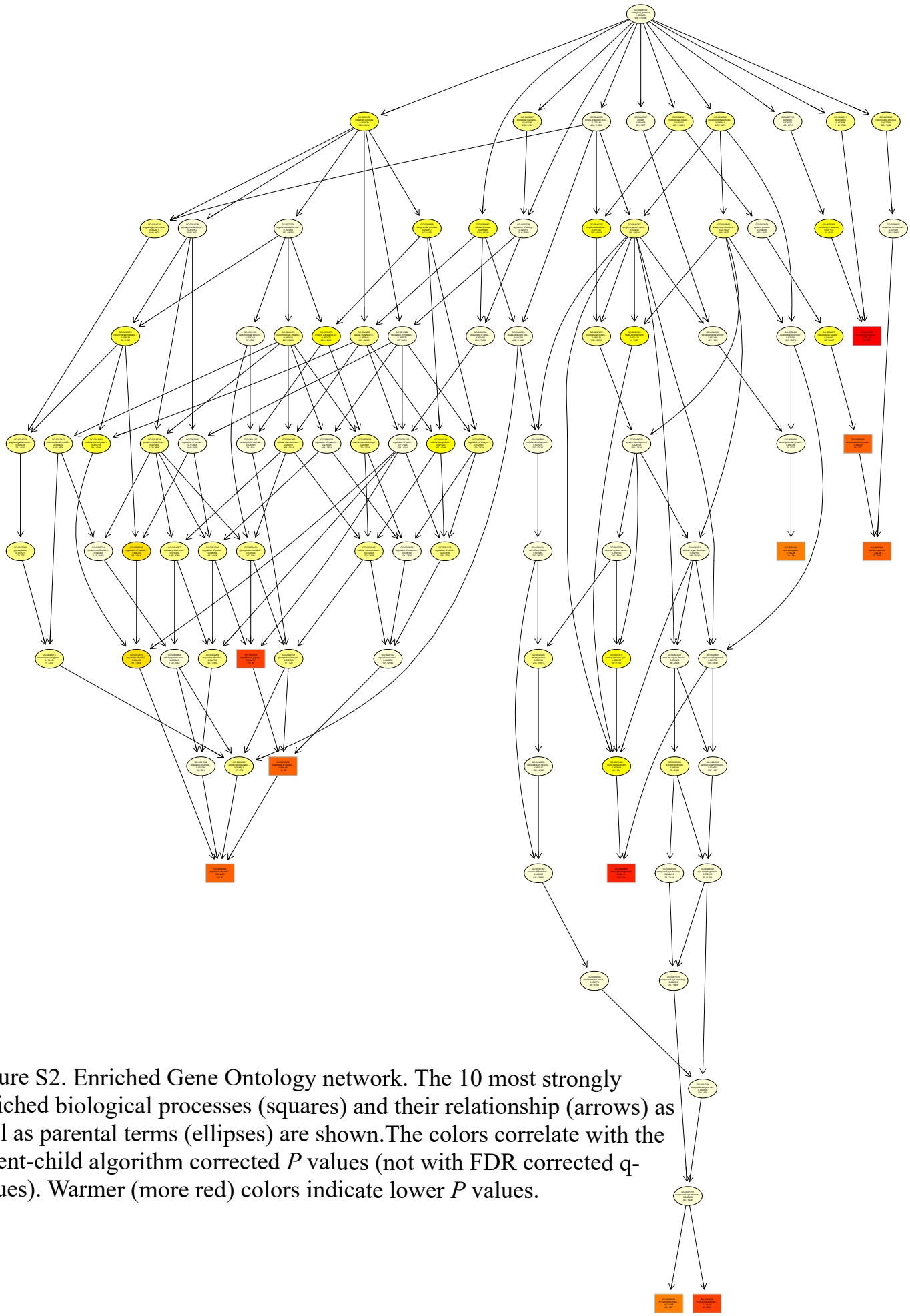

Figure S2. Enriched Gene Ontology network. The 10 most strongly enriched biological processes (squares) and their relationship (arrows) as well as parental terms (ellipses) are shown.The colors correlate with the parent-child algorithm corrected *P* values (not with FDR corrected q-values). Warmer (more red) colors indicate lower *P* values.